National Institute of Standards and Technology detector-based photometric scale

C. L. Cromer, G. Eppeldauer, J. E. Hardis, T. C. Larason, and A. C. Parr

The Système International base unit for photometry, the candela, has been realized by using absolute detectors rather than absolute sources. This change in method permits luminous intensity calibrations of standard lamps with an expanded uncertainty of 0.46%, almost a factor-of-2 improvement. A group of eight reference photometers has been constructed with silicon photodiodes, matched with filters to mimic the Commission Internationale de l'Éclairage spectral luminous efficiency function for photopic vision.The design, characterization, calibration, evaluation, and further application of the photometers are discussed.

Key words: Calibration, candela, illuminance, lumen, luminous intensity, lux, measurement, photometer, photometry, scale, standards, units.

1. Introduction

Traditionally standardization in photometry was a discipline driven by primary light sources, first candles, then flames,[1] carbon-filament lamps, and, beginning in 1948, blackbody radiators operated at the freezing-point temperature of molten platinum.[2] The latter marked a turning point, as the platinum-point blackbody, valued for its reproducibility and universality compared with the earlier alternatives, was the first standard photometric source whose radiometric properties in principle could be readily calculated.

Over time, dissatisfaction with platinum-point blackbody standards grew. For the few national laboratories that had them, they were difficult to maintain. They operated at a temperature of little technological interest [taken first as 2045 K, later 2042 K, in the International Practical Temperature Scale of 1968 (IPTS-68)], and the applicability of this broadband radiation to spectroradiometry was poor. In 1975, Blevin and Steiner,[3] reflecting the mood of the period, made two proposals. They sought first to redefine the photometric base unit in a manner to fix its relationship with other Système International (SI) base units, such as the second and the ampere. Second, they argued that the photometric base unit should be changed from the candela to the lumen, considering the close relationship between luminous flux (lumens) and radiometric power measurement (watts).

After additional study and due consideration, in 1979 the 16th Conférence Générale des Poids et Mesures adopted the first of these proposals. They abrogated the definition of the candela (originally called the new candle) first adopted by the Eighth Conference in 1948 and decided the following[4]:

"The candela is the luminous intensity, in a given direction, of a source that emits monochromatic radiation of frequency 540×10^{12} hertz and that has a radiant intensity in that direction of (1/683) watt per steradian."

Since then, national standards laboratories have been free to realize the candela by use of whatever radiometric means they found most suitable. At the National Institute of Standards and Technology (NIST) [then National Bureau of Standards (NBS)] the luminous intensity scale remained based on a standard source, a blackbody radiator operating at the freezing-point temperature of molten gold (the gold point).[5] The blackbody radiation at the gold point (1337.58 K in IPTS-68) was used to calibrate a variable temperature blackbody, which provided the NBS scale of spectral radiance.[6] From this the spectral irradiance scale was derived.[7] The luminous intensity scale was realized through spectral irradiance measurements of candela lamps forming a

The authors are with the Radiometric Physics Division, Physics Laboratory, Technology Administration, National Institute of Standards and Technology, U.S. Department of Commerce, Gaithersburg, Maryland 20899.

Received 27 April 1992.
0003-6935/93/162936-13$06.00/0.
© 1993 Optical Society of America.

primary reference group. A secondary reference group of candela lamps, calibrated against the primary group, was used for routine calibrations.

All the measurements in this lineage compared a light source with another light source. The final measurement uncertainty of 0.8% (2σ) (Ref. 8) contained a relatively large component from the uncertainty in the gold-point temperature at the top of the chain (when IPTS-68 is compared with thermodynamic temperature), and it was further limited by the long-term behavior of the incandescent lamps that were used.

In 1990 the introduction of the new International Temperature Scale (ITS-90) caused changes. The gold point was redefined as 1337.33 K,[9] which caused the NIST luminous intensity scale to shift, depending on the color temperature of the source, by $\sim 0.35\%$.[10] More important, NIST revised its procedures to decouple the spectral radiance scale from ITS-90. NIST now considers the gold-point temperature to be a measured rather than a defined quantity. While the current NIST measurement of 1337.33 ± 0.23 K (Ref. 11) is in exact agreement with ITS-90, the new policy allows for the possibility of future scale revisions as experimental information becomes available. The current NIST gold-point temperature of 1337.33 K is detector based. That is, the result follows from measurements with absolute radiometric detectors, a silicon photodiode and an electrically calibrated radiometer.

The purpose of this paper is to describe the considerable simplification that results by realizing the candela against the detector base directly and to announce a new NIST scale for luminous intensity. The benefits of this conversion include much improved precision in our calibration services. Additionally, we are motivated by the increased flexibility that permits us to provide customers routinely with calibrated detectors as well as calibrated lamps.

2. Experimental Approach

The 1979 redefinition of the candela permitted many different methods to be used to derive a photometric scale. All rely on the principles governing photometry as compiled by the Bureau International des Poides et Mesures (BIPM),[12] most notably the spectral luminous efficiency function for photopic (cone) vision $V(\lambda)$, which relates visual sensitivities at different wavelengths.[13] (The lone frequency of 540×10^{12} Hz mentioned in the definition has a wavelength of 555.016 nm in standard air, which for almost all purposes can be taken to be 555 nm without affecting the accuracy of a real measurement.)

Different national laboratories[5,14–20] and other research facilities[21] have employed various techniques to realize the candela scale. Most have used detectors that were equipped with filters that were designed to match their spectral responsivity to the $V(\lambda)$ function, as do we. Many have used absolute radiometers, such as electrically calibrated thermal detectors and self-calibrated silicon photodiodes. However, we chose to use calibrated silicon photodiodes because of their wider dynamic range and simplicity of operation.

A. Mathematical Framework

The photometric analog of power in radiometry is luminous flux Φ_v, where

$$\Phi_v(\mathrm{lm}) = K_m \int_\lambda \Phi_e(\lambda) V(\lambda) \mathrm{d}\lambda, \tag{1}$$

$\Phi_e(\lambda)$ is the incident spectral power distribution of the light (watts per nanometer), and K_m is the proportionality constant in the definition of the candela. While a strict reading of the definition gives $K_m = 683.002$ lm/W,[13] for almost all purposes it is taken to be 683 lm/W without affecting the accuracy of any real measurement.

A photometer measuring this flux has an output current,

$$I(\mathrm{A}) = \int_\lambda \Phi_e(\lambda) s(\lambda) \mathrm{d}\lambda, \tag{2}$$

where $s(\lambda)$ is its spectral responsivity. It is advantageous to factor

$$s(\lambda)(\mathrm{A/W}) = s(555) s_n(\lambda), \tag{3}$$

where $s(555)$ (amperes per watt) is the value of $s(\lambda)$ at 555 nm. This emphasizes the similarity of $s_n(\lambda)$ to $V(\lambda)$, both dimensionless functions that peak at [or in the case of $s_n(\lambda)$ near] 555 nm. It also permits the overall uncertainty of the spectral responsivity scale to be associated with one number, $s(555)$, with the function $s_n(\lambda)$ consisting of relative measurements only.

The luminous responsivity[22] of the photometer

$$s_v(\mathrm{A/lm}) = \frac{I}{\Phi_v} = \frac{s(555)}{K_m} \frac{\int_\lambda \Phi_e(\lambda) s_n(\lambda) \mathrm{d}\lambda}{\int_\lambda \Phi_e(\lambda) V(\lambda) \mathrm{d}\lambda}. \tag{4}$$

For a perfect photometer, $s_n(\lambda)$ would equal $V(\lambda)$, and its luminous responsivity would be independent of the power distribution of the light. In practice this approach requires knowledge of $\Phi_e(\lambda)$ for a spectral mismatch correction factor to be calculated:

$$F = \frac{\int_\lambda \Phi_e(\lambda) V(\lambda) \mathrm{d}\lambda}{\int_\lambda \Phi_e(\lambda) s_n(\lambda) \mathrm{d}\lambda}. \tag{5}$$

In general, the closer $s_n(\lambda)$ is to $V(\lambda)$, the better F will be known for the same incertitude of $\Phi_e(\lambda)$.

Figure 1 illustrates the application of such a pho-

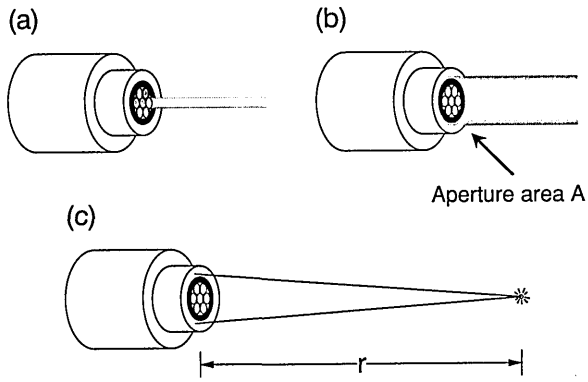

Fig. 1. Application of a photometer to luminous intensity measurement as a progression. (a) When the light beam underfills the entrance aperture, the photometer measures luminous flux (lumens), the photometric analog to radiant power. The responsivity of our detectors was tested in at least seven positions, as shown. (b) When the light beam overfills the entrance aperture, the photometer measures illuminance [lux, (lumens per square meter of the aperture)]. (c) When the photometer is used with a point light source at a distance, the aperture area and the distance to the source combine to define a solid angle. The photometer then measures the luminous intensity [candela (lumens per steradian)] of the source.

tometer to luminous intensity (candela) measurement. In Fig. 1(a) it is supposed that the photometer intercepts a beam of light, and that all the light illuminates only a portion of the active area of the photometer. In this case the photometer would have an output current I from which the luminous flux of the beam could be determined, presuming that $s(\lambda)$ is sufficiently invariant from point to point over the active area:

$$\Phi_v(\mathrm{lm}) = \frac{K_m F I}{s(555)}. \tag{6}$$

In Fig. 1(b), it is further supposed that the photometer is fitted with an aperture of precisely known area. Then, if the light is not confined to a small spot but rather overfills the aperture reasonably uniformly, the photometer would have an output current I that is proportional to the illuminance E_v [lux (lumens per square meter)] on the aperture. For an aperture area A (square meters),

$$E_v(\mathrm{lx}) = \frac{K_m F I}{s(555)A}. \tag{7}$$

Figure 1(c) shows the overall geometry for luminous intensity measurement. A point light source a distance r from the plane of the aperture and lying on the normal to its center would have a luminous intensity of

$$I_v(\mathrm{cd}) = \frac{K_m F I r^2}{s(555)A}. \tag{8}$$

The applicability of these geometric prerequisites to real measurements is explored below.

B. Description of the Photometers

To measure photometric quantities and to maintain the candela scale at NIST, a group of eight photometers has been developed. They contain $V(\lambda)$ matching filters as well as specially selected silicon photodiodes and the electronics to implement the high-sensitivity, wide-dynamic-range circuit previously described.[23] With an integration time of 1.67 s, a measurement bandwidth of 0.3 Hz, and an amplifier gain of 10^{11} V/A, the output voltage noise in these devices corresponds to ~ 1 fA of photocurrent. This important feature of the NIST detectors permits precise measurement of $s_n(\lambda)$ even in the wings of the peak.

Figure 2 depicts the photometer design. The silicon photodiode, the $V(\lambda)$ correcting-filter package, and a precision aperture are mounted in the front piece of a cylindrical housing. A Teflon disk of low electrical conductivity supports the photodiode; small pin terminals in the disk form a socket. The $V(\lambda)$ filter is glued to a holder and is positioned close to the photodiode. On the front side of the filter the precision aperture is glued to a holder. This holder is carefully machined so that its front surface, the frontmost surface of the photometer, is 3.00 mm from the plane of the aperture knife edge. All these components are marked in a manner that allows us to preserve their orientation during disassembly and reassembly.

The cylindrical housing itself, which extends back from the front piece shown in Fig. 2, contains an amplifier that also acts as a photocurrent-to-voltage converter. A switch selects the transimpedance gain of the amplifier, decade values from 10^4 through 10^{10} Ω. (Photometers 1 and 2 also have a 10^{11}-Ω range.) The characteristics of the filter and photodiode change with temperature, so the operating temperature of the photometer is monitored by a sensor inserted in the front wall of the housing.[24] The housing contains all additional components necessary for signal and temperature outputs; it is lighttight and acts as an electrical shield.

C. New Candela Scale

The candela-scale realization is simplified when this approach is used. The scale is derived by measuring $s(\lambda)$ of each photometer in the group directly against the NIST spectral response scale. The spectral response scale is derived from comparative measurements against absolute radiometric detectors; at the time of this study, 100% quantum efficient detectors[25] were the basis of the scale. With the application of the Commission Internationale de l'Éclairage (CIE) $V(\lambda)$ curve in Eq. (5) and the application of the geometric definitions in Eq. (8), the candela is determined. Additionally, since the photometers do not age in use as rapidly as lamps do, an additional step to form a working group of photometers for routine use was unnecessary.

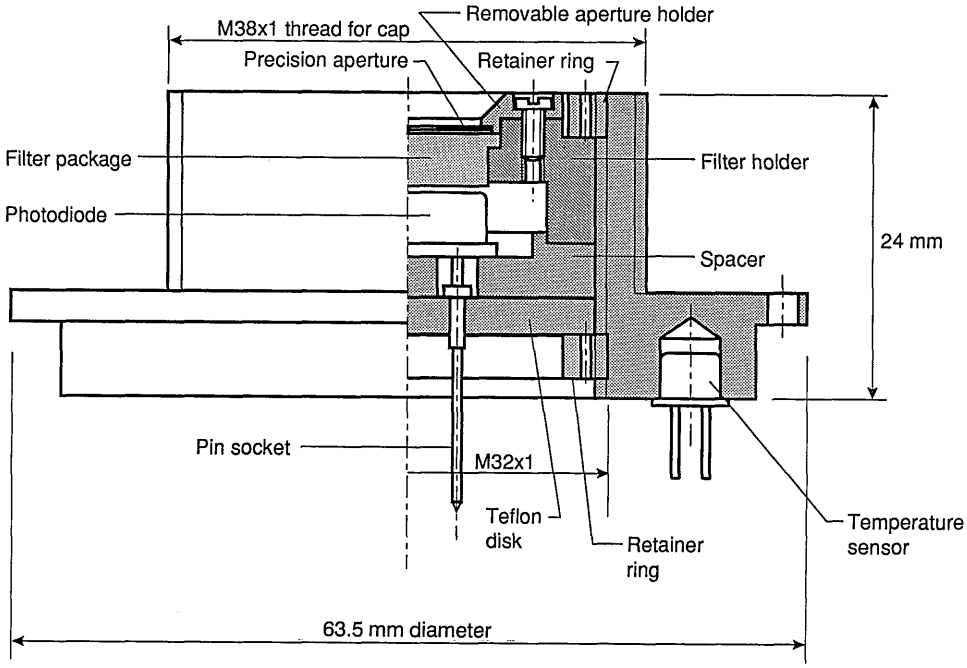

Fig. 2. Photometer design. A filter modifies the spectral response of a silicon photodiode to replicate as closely as possible the 1924 CIE Spectral Luminous Efficiency Function for Photopic Vision.

3. Characterization of the Photometers

A. Instrumentation and General Procedures

The principal apparatuses used to study the photometers and their components comprise the Spectral Comparator Facility (SCF), which holds the NIST spectral response scale. A UV instrument spans 200–400 nm; a visible/near-IR instrument spans 400–1800 nm. As shown in Fig. 3 a detector under test is held in a carriage that can be translated under computer control. Any point on the active area of the detector can be positioned at the focus of a 1.1-mm, nearly circular spot from a monochromator. The carriage also holds reference detectors that serve as secondary standards and that are measured alternately with the device being tested. Compensation for changes in the light source during the course of the measurement is made by using the signal from a monitor detector. The computer controls the monochromator, which has a bandpass of 4 nm for this spot size and a spectral accuracy of ±0.2 nm.[26] The apparatuses typically deliver a few microwatts of optical power to the detector.

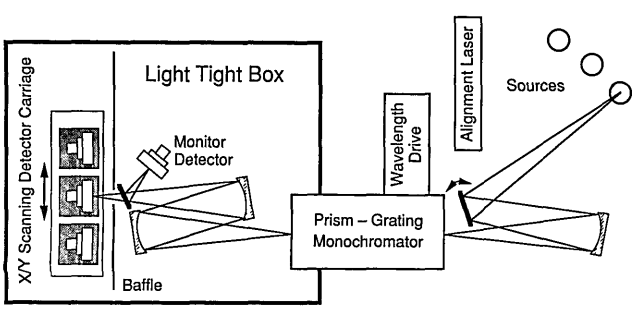

Fig. 3. Facility used to calibrate the photometric detectors with visible and IR radiation. The UV instrument is similar.

Care was taken to insulate thermally the devices from the carriage, which heats up during use because of its stepping motors. The ambient temperature during measurement was monitored; when applicable the temperature circuitry of the device under test was used. This permitted a direct comparison between the temperatures at calibration and use. Generally variations in ambient temperature were held within ±1 °C during the course of a measurement.

In addition to the optical calibrations performed at the SCF, the transimpedance gains of the photometer amplifiers were calibrated electrically. With this procedure the photodiode is replaced by a computer-controlled voltage source V_{IN} and a resistor substitution box in series. Unlike the internal resistors R_f built into the photometer heads, the external resistors R_{EXT} are easily measured. (As explained in Ref. 23, R_f is the transimpedance gain of the amplifier.) For many combinations of internal and external resistors (as selected by the photometer gain switch and the substitution box, respectively), the output of the photometer V_{OUT} is measured for a series of V_{IN}. The linear coefficient of this dependence, as best fitted, is equal to the corresponding R_f/R_{EXT}. This permits the individual values of R_f to be determined to an accuracy of better than 0.01%. Calibrations on the SCF, reported in volts per watt for an individual photometer gain-switch setting, can be transferred between different settings when these data are used.

B. Component Characterization

Before the photometers were assembled, the SCF was used to study their components, both to diagnose

systematic effects and as the basis for aging studies. When the spectral response of an individual photodiode or a photometer (the photodiode, filter, and aperture together) was measured, the device itself was mounted on the carriage. For the spectral transmittance of a filter alone to be determined, the filter was held on the carriage, but a photodiode behind it was not. (Filter transmittance is the ratio of the apparent detector responsivity with and without the filter interposed in the beam.) In this case the photodiode was tilted to prevent interreflections.

For this project we used Hamamatsu S1226 and S1227 series photodiodes.[27] They were selected for the largest shunt resistance that the manufacturer could provide, 2.5–7.0 GΩ, so that noise and drift in the circuit could be minimized.[23] This type of photodiode has less IR sensitivity than some others, which is advantageous for photometry. As a consequence the IR response is more temperature dependent than the alternatives. We used quartz rather than glass or resin windows, since we found that the former had less surface scatter. Photodiodes with a 1-cm^2 area were used in photometers 1 and 2 because they contained larger $V(\lambda)$ filters; the other photodiodes were 0.3 cm^2.

The spectral responsivities of these photodiodes were measured on a grid of points 0.5 mm apart to determine the spatial uniformity of the photodiodes and to screen for defects. Within the portion exposed through the aperture, the uniformities were generally constant to better than 0.2%. The change in responsivity caused by changes in temperature, for 400–700 nm, was $< 0.03\%/°C$.

We obtained layered, colored glass filters from various sources to benefit from the experience that this diversity offers. Filters 1 and 2 were provided through the courtesy of the National Research Council of Canada (NRC), filter 3 was provided courtesy of the National Physical Laboratory of the U.K. (NPL), and filters 4–8 were manufactured by PRC Krochmann (PRC).[28] For a good realization of the $V(\lambda)$ curve, such filters are individually made. First, the glasses are carefully chosen,[14,29] and then the thicknesses of the individual glass layers are determined through an iterative procedure including repeated polishing and transmittance measurements. Filters 1 and 2 were originally designed to match the QED-200 trap detector; filter 3 was designed to match Centronics OSD 300-5 photodiodes. Filters 4–8 were optimized to match our type of silicon photodiode.

While spectral match is important, so that Eq. (5) is insensitive to $\Phi_e(\lambda)$, other important filter properties include spatial uniformity, temperature dependence, and birefringence. Filters 4–8 were selected from among 24 candidates after visual inspection. Filters with obvious dislocations, scratches, bubbles, and other optical defects were rejected. The remaining filters were screened for uniformity by scanning them with a white-light spot 1.5–2.0 mm in diameter. Those with the sharpest and largest changes were eliminated.

After initial selection more detailed diagnostics were performed. Transmittance measurements were made in 5-nm intervals and at many positions on the filters to determine their spatial uniformity. The temperature dependence of the filter transmittance was estimated with a commercial spectrophotometer equipped with a sample heater.

Since the filters are composed of dissimilar layers cemented together, any resulting strains might cause birefringence or a polarization-dependent transmittance. (The light from a monochromator during calibration is partially polarized.) To verify the absence of such a problem, representative filters were tested. A plane polarizer was interposed between the photometers and a lamp operating at ~2856 K. No change in signal above noise was noted as the photometer was rotated, limiting the potential error to ~0.01%. Nevertheless, candidate filters that showed the greatest birefringence were also rejected.

The photometers were fitted with precision apertures, nominally 0.5 cm^2 for photometers 1 and 2 and 0.1 cm^2 for photometers 3–8. They were electroformed with nickel-clad copper and given a black, nickel finish. The fabrication and properties of similar apertures are discussed in Ref. 30. Most important to us is the resultant knife edge from this process, sharp and without burrs. However, such apertures may depart from circularity.

The Precision Engineering Division at NIST measured and certified the areas with a View Engineering Precis 3000 vision-based measuring machine.[31] After a pass was made to find the approximate center of the aperture, 720 radii were measured from the center to the lip at 0.5° angular intervals. The measurements were not sensitive to the method of lighting the aperture (i.e., different forms of front and back lighting). From these radii the area was estimated by a polygonal approximation. The combined uncertainties of the radii measurement and the area estimation were given at 0.02% for the larger apertures and 0.05% for the smaller. Since the coefficient of linear thermal expansion for copper is ~0.0017%/°C, temperature corrections are unnecessary for this study.

C. Photometer Characterization

After the photodiodes, filters, and apertures were individually tested, they were assembled into photometers as shown in Fig. 2. The advantage to calibrating the components assembled is that internal reflections and scattering have similar effects during both calibration and use. The essential role of the SCF is to calibrate the spectral responsivity $s(\lambda)$ of the photometers to determine $s(555)$ [Eq. (3)] and F [Eq. (5)]. The small output spot from the SCF can be positioned at various places within the aperture.

$s(\lambda)$ Was measured at 5-nm intervals at one position near the center of the aperture of each photometer. Data from representative photometers are shown in Fig. 4(a). Of particular importance in these data is the degree of IR and UV suppression, the latter including both transmission and fluorescence signals.

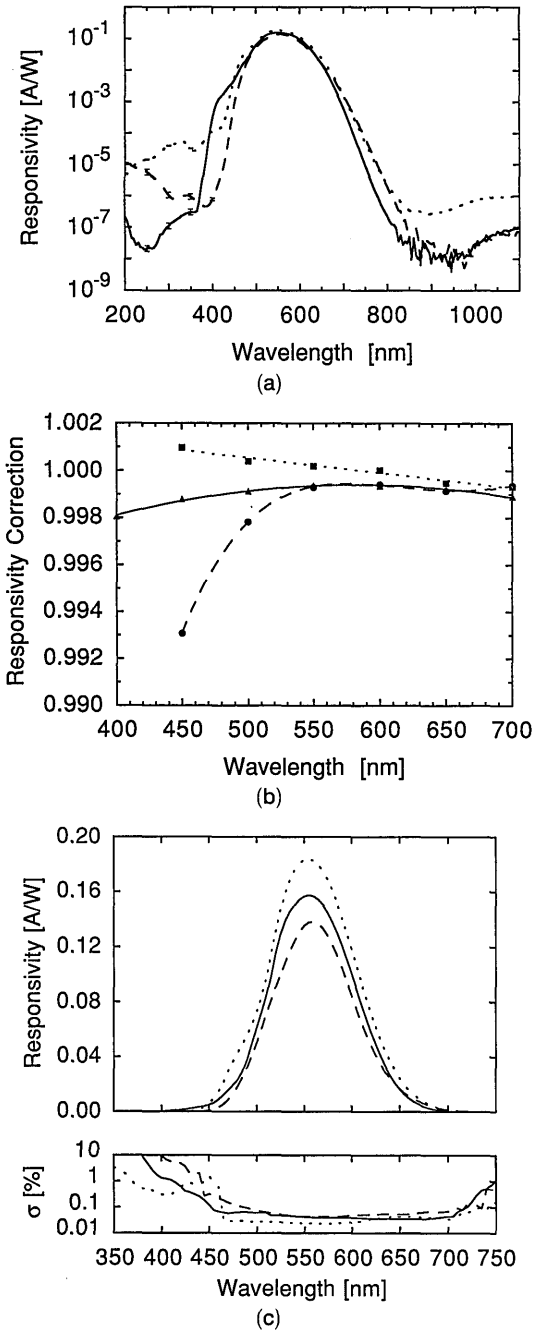

Fig. 4. (a) Responsivity of the filtered photodiode packages with emphasis on their behavior in the UV and IR. One spot in the center of the aperture is probed. The estimated error at this spot is commensurate with the width of the curve in the visible, with the apparent scatter of the data in the IR, and shown by error bars in the UV. Representative packages: photometer 2, NRC, dashed curve; photometer 3, NPL, dotted curve; photometer 5, PRC, solid curve. (b) Comparison of responsivity at the center spot to the average of many spots over the face of the aperture. Data taken at 50-nm intervals are interpolated by polynomial fits. The correction factor converts the responsivity at the center to the average responsivity over the face of the aperture. The curves are as in (a). (c) Responsivity of the filtered photodiode packages. The curves are as in (a) after the correction in (b) has been applied.

However, a correction was needed because $s(\lambda)$ varied over the aperture area. The spectral responsivity of each photometer, relative to the center point, was determined at 50-nm intervals on a fine, rectangular mesh of points. For the larger apertures (photometers 1 and 2) the step size was 0.25 mm; for the smaller apertures (photometers 3–8) the step size was 0.2 mm. Measurements that were not affected by the aperture edge were averaged.

Figure 4(b) shows such data, the ratio of the average responsivity to the datum from the center spot. From these ratios fits are made to polynomials, which are taken to be correction factors, transformations from the responsivity data at the center point to the responsivity over the whole aperture. After application to the data in Fig. 4(a) the final spectral responsivities for representative photometers are shown in Fig. 4(c). The scatter given in the lower part of the figure is only the statistical noise of measuring $s(\lambda)$ at the center. Additional uncertainties also apply; for example, the responsivity variation over the mesh helps to determine the error that might arise if the aperture is not fully and uniformly illuminated. During the calibration process the temperature of a photometer was monitored by its built-in thermometer. Variations were generally held to ± 1 °C.

$s(\lambda)$ Varies with the temperature of the photodiode and, even more so, the filter. We measured the overall temperature effect by operating representative photometers at elevated temperatures. The photometers were placed in a heated, plastic foam box and allowed to reach thermal equilibrium overnight. They were illuminated in the normal manner by an inside-frosted lamp of the type normally used at NIST for luminous intensity calibrations. The lamp had a color temperature of ~ 2856 K. A temperature-controlled monitor detector with a $V(\lambda)$ filter compensated for the variation in lamp output from lighting to lighting.

The photometer responsivities [I/E_v as in Eq. (7)] decreased with increasing temperature, as measured with each photometer's built-in thermometer. Compared with the value when the photometer was unheated, the responsivity of photometer 3 decreased by 0.049%/°C, the responsivity for photometers 1 and 2 decreased by 0.063%/°C, and the rest decreased by 0.088%/°C, the standard uncertainty of these results being $<0.002\%/°C$. The temperature effect would be different when sources are measured with other spectral compositions.

In Table 1 pertinent aspects of the photometers are summarized. As explained in Ref. 23, the higher the shunt resistance of the photodiode, the better can be the signal-to-noise ratio of the circuit. The limiting photocurrent noise of ~ 1 fA in photometers 1 and 2 corresponds to a limit sensitivity of $\sim 10^{-7}$ lx. Besides the spectral correction factor F a traditional metric of the match of $s_n(\lambda)$ to $V(\lambda)$ is f_1',[22] which is also shown in the table.

When an actual lamp is used, its color temperature

Table 1. Summary of the Photometers

Photometer	Photodiode	Shunt Resistant (GΩ)	Filter Source	Calibration (nA/lx)	F (2856 K)	f_1' (%)
1	S1227-1010BQ	5.0	NRC	10.116	1.002	6.00
2	S1227-1010BQ	5.2	NRC	10.067	1.003	5.97
3	S1226-8BQ	7.0	NPL	2.821	0.954	7.26
4	S1227-66BQ	6.6	PRC	2.350	0.990	2.55
5	S1226-8BQ	7.0	PRC	2.335	0.989	2.35
6	S1226-8BQ	7.0	PRC	2.331	0.990	2.37
7	S1226-8BQ	7.0	PRC	2.341	0.987	2.79
8	S1226-8BQ	4.3	PRC	2.334	1.000	1.43

may be other than the desired 2856 K. Figure 5 shows the sensitivity of F to variations in blackbody temperature for the different types of filter used.

D. Illuminance Accuracy

Following Eq. (7), the combined standard uncertainty u_c of the illuminance responsivity of the photometers (I/E_v) arises from the uncertainties in $s(555)$, F, and A. They are summarized in Table 2. By adopting the terminology of BIPM (Ref. 32) and ISO,[8] the uncertainties are categorized as Type A, those that arose from the statistics of repeated measurements, and Type B, those that did not (such as estimates of possible systematic effects).

The principal uncertainty in $s(555)$ is that of the accuracy of the NIST spectral response scale. The currently accepted value of 0.11% (Ref. 33) arises largely from the uncertainty in the absolute spectral response of silicon photodiode trap detectors, with smaller additional contributions resulting from comparisons between the trap detectors and the working standards.

A number of smaller uncertainties arise in the determination of F, which is to say that these effects are not material to the accuracy of the illuminance scale. They are also listed in Table 2 and include the measurement scatter shown in Fig. 4(c), the procedure of deriving Fig. 4(c) from Figs 4(a) and 4(b), the presumption that $\Phi_e(\lambda)$ of actual lamps can accurately

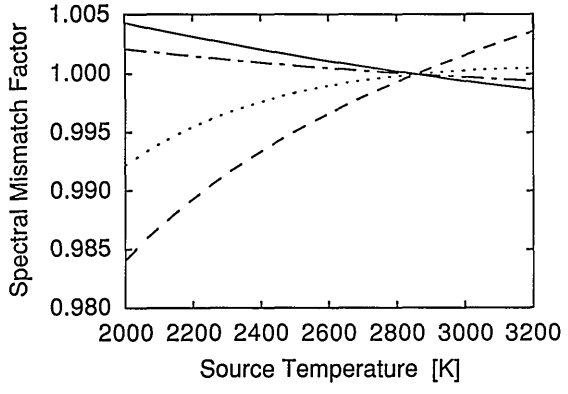

Fig. 5. Effect on photometer calibration when sources at different temperatures are viewed. The required correction is reported as $F(\text{Temp})/F(2856\text{ K})$. Representative packages: Photometer 2, dashed curve; photometer 3, dotted curve; photometer 5, solid curve; photometer 8, dashed–dot curve.

replicate and be represented by CIE Source A (a Planckian radiator at 2856 K), and the residual responsivity of the photometer beyond the domain of $V(\lambda)$ in the UV (200–360 nm) and IR (830–1100 nm).

Two experimental factors on the SCF affect the responsivity through both $s(555)$ and F. A wavelength calibration uncertainty of 0.2 nm leads to a responsivity uncertainty of 0.14%, and the effect of the $f/9$ optics (rays at different angles being attenuated differently by the filter) would lead to a bias of the same magnitude. To improve accuracy, we used both the SCF and the NIST Reference Spectrophotometer[34] to measure the transmittance of the $V(\lambda)$ filters. Comparison of the data, matching peak position and shape, indicated that the two sources of error on the SCF fortuitously canceled each other. The residual uncertainty in responsivity caused by the wavelength scale is 0.04% and caused by the SCF optics is 0.05%.

Although the aperture areas were measured and certified to the accuracy shown in Table 2, these measurements were made while the apertures were detached. We also sought to confirm their behavior when they were installed in the photometers. For this we used the SCF and scanned its small beam over the face of the photometer. The positioning stage provided a length scale, although not a calibrated one. While the details of this test are beyond the scope of this paper, we were surprised to find that the effective areas of the nominally 0.1-cm^2 apertures were on average 0.36% larger. This cannot be fully accounted for by temperature variations, responsivity variation within the aperture, an inaccuracy of the translation scale, or the optics of the SCF. Numerical modeling indicates that a small portion of it may arise from reflections and scattering within the photometer, where the back side of the aperture traps light that would otherwise escape. The Precis 3000 measurements differed on average by only 0.01% from independent measurements made by the aperture manufacturer; the accuracies of the actual aperture areas are not in doubt. Rather there may be an unaccounted aspect of the photometers themselves.

Additional small uncertainties arise from the method of temperature correcting the photometers, from potential polarization selectivity of the photometers, from the electrical calibration of the amplifier, and from the system linearity. Random influences in this budget (of both Types A and B) together cause

Table 2. Uncertainty Budget for Illuminance Calibration

Measurable	Uncertainty Origin	Uncertainty (%) Type A	Uncertainty (%) Type B
$s(555)$			
	Spectral responsivity scale		0.11
	Comparison of photometer to scale	0.04	
F			
	Measurement scatter (noise)	0.01	
	Data fitting procedure	0.01	
	Residual nonuniformity within aperture	0.02	
	Color temperature of lamp (±10 K)		0.02
	Planckian approximation for lamp		0.02
	IR leakage		0.003
	UV leakage and fluorescence		0.002
Correlated $s(555)$ and F			
	Wavelength calibration		0.04
	Numerical aperture		0.05
A			
	Aperture area (as certified, small apertures)		0.05
Additional			
	Temperature variation		0.03
	Polarization sensitivity		0.01
	Electrical current-to-voltage conversion	0.003	
	Responsivity nonlinearity		0.001
	Other	0.12	
Combined standard uncertainty		0.19	
Expanded uncertainty ($k = 2$)		0.39	

an uncertainty of ~0.06%. However, an intercomparison among the eight photometers, after calibration, found a self-consistency of 0.13%. An additional 0.12% is added to the budget to account for other influences.

4. Realization of the Candela

A. Photometry Bench

The application of a photometer, measuring illuminance, to the luminous intensity determination of a light source [Eq. (8)] is facilitated by the optical bench shown in Fig. 6. The base consists of three 1.8-m-long, 46-cm-thick, steel optical tables with a regular array of tapped holes. Upon it, rigid telescope mounts and upright, marked fiducial plates define the reference axes. The longitudinal axis runs parallel to rails upon which a carriage glides, holding a photometer. A support with cross hairs is substituted for the photometer to align the carriage and rails; lateral alignment within ±2 mm is achieved at the end opposite the telescope. By substituting a flat mirror for the photometer and by viewing the telescope in itself, orthogonality is ensured to within 5 mrad. A lamp being measured is mounted on another carriage, which allows it to be placed at the intersection of the reference axes. With a side-viewing telescope, the lamp filament is aligned to the plane defined in combination with the vertical fiducial mark. (When frosted lamps are measured, such as the type normally issued by NIST as luminous intensity standards, a model is aligned rather than the lamp itself. The model contains additional fiducial marks both to set the filament plane and to locate the filament within that plane.[5])

The lamp is powered by a constant-current source, which is set under computer control with a resolution of 0.15 mA. The current is independently monitored across an air-cooled, Leeds & Northrup 4360, 0.1-Ω precision shunt resistor,[35] which is calibrated at NIST in operating conditions to an accuracy of 0.002%. The proper operating current for the color temperature of interest is determined initially by finding the proper ratio of the signals from red- and blue-filtered detectors. Additionally, the computer monitors the lamp voltage and the photometer signal and temperature, and it operates the shutter under programmed control.

The apparatus in Fig. 6 is covered by a plastic box lined with black velvet. Surfaces within the box, to the maximum extent possible, are either painted black or covered with black cloth. A baffled chimney above the lamp allows for convective cooling without introducing stray light. A light trap is interposed in front of the longitudinal telescope during operation to minimize the light that is reflected back at the photometer. (The side telescope is blocked by black cloth.)

To estimate the magnitude of stray light resulting from reflections and scattering, an additional photometer was used concurrently during testing and evalua-

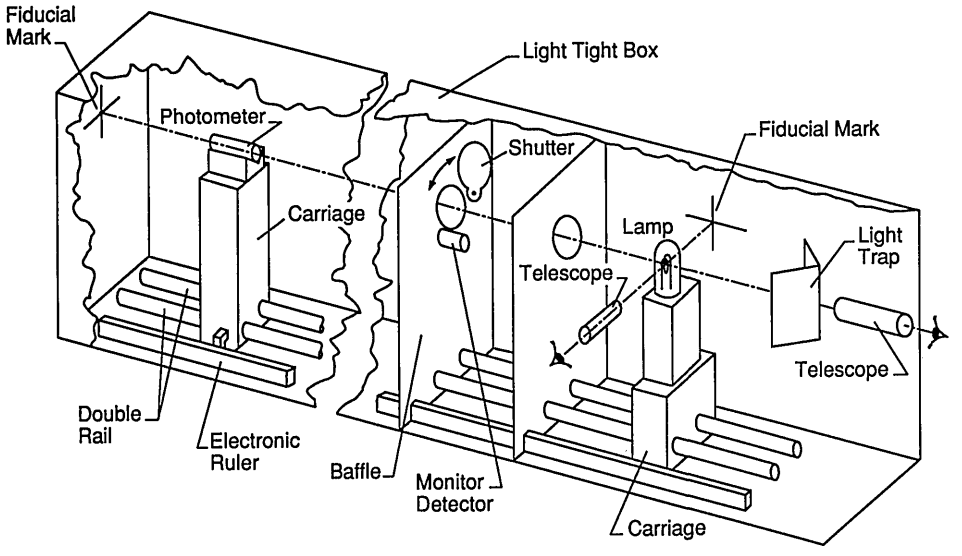

Fig. 6. New NIST photometry bench.

tion. It was placed outside the area illuminated through the baffles, but near, and oriented in the same general manner as, the photometer being used for measurement. With various arrangements the stray light was consistently $<0.03\%$ of the signal. To estimate the stray light originating near the lump, we covered the side of the lamp toward the photometer. This signal was $<0.001\%$ of the original. The box attenuated the ambient light from the laboratory by $\sim 10^6$.

B. Lamp-to-Photometer Distance

The position of the photometer carriage is monitored by a computer-readable, absolute linear encoder with a resolution of 0.013 mm. The distance r between the photometer and the transverse reference axis, and a lamp filament, is fixed by sliding an attachment on the photometer carriage into the view of the telescope so that the zero position can be noted. The accuracy of the encoder was checked with a 2.75-m vernier caliper by moving the photometer carriage to various positions and measuring its distance mechanically from the telescope mount as well as electronically. These repeated measurements had a consistency between the methods of 0.18 mm, which we take to be the uncertainty in determining the distance. In actuality most of this scatter was associated with the use of the large caliper, and it will not affect photometric measurements. An uncertainty of 0.18 mm in separation corresponds to an uncertainty in luminous intensity of 0.01% when the photometer is at the far end of the bench.

More significantly, a lamp is not the point source envisaged in Fig. 2(c). The size of the radiating volume requires that I_v in Eq. (8) be taken as the asymptotic value at large r. Typical inside-frosted lamps calibrated at NIST are tubular with a radius of 5 cm and extend 10 cm below the center of the filament, which is 5 cm below the top of the lamp. Less important is the transverse extent of the radiating and scattering surfaces away from the longitudinal axis. At a distance of 2 m to the photometer, a lateral displacement of 10 cm by a point source would decrease its reading by only 0.38% (0.25% because of the increased distance and 0.13% because of the increased angle of incidence). In comparison a 5-cm longitudinal displacement of a point source would affect the reading by 5%. Clearly the model is most sensitive to the longitudinal location of the origin of the light.

For this study the automation afforded by computerized instrumentation and data analysis allowed us to make rapid measurements with the photometer at many distances from the lamp. Lamp intensity fluctuations were accounted for by a stationary, unfiltered, temperature-controlled silicon photodiode. In this way an effective origin of the light was found as the best-fit offset r_0 in the expression

$$E_v = \frac{I_v}{(r - r_0)^2}, \tag{9}$$

given the measured illuminance E_v (as corrected) as a function of r. (Similarly the best-fit luminous intensity I_v can be derived.)

Typical offsets of 0.50 ± 0.15 cm were found for NIST inside-frosted lamps, with a systematic tendency for the offset to decrease by ~ 0.15 cm after a lamp had been burning for ~ 1 h. This may be attributed in part to imperfect compensation by the monitor if the spectral distribution of the lamp was changing, particularly in the IR. Surprisingly, similar offsets of 0.3 ± 0.2 cm were found in a set of five, unfrosted Osram WI 41/G lamps. However, part of this (<0.2 cm) can be attributed to the shape and thickness of the glass envelope, which, acting as a diverging lens, displaces the apparent position of the filament.

The uncertainty of r in Eq. (8) is dependent both on

the physical measurement of distance and on the applicability of the model Eq. (8) represents, that is, on how one wishes to treat the issue of the effective origin of the light. To ignore it means including a potential systematic error in r; to measure it means using up precious hours of a standard lamp's life. For the purpose of defining the new NIST scale of luminous intensity, we presume that the offset is determined and applied, either for the lamp being measured or from a collection of lamps of similar construction. $u_c(r)$ is then dominated by the uncertainty in the offset distance, typically 0.11 cm in our measurements. At $r = 3.7$ m the corresponding uncertainty in luminous intensity is 0.06%.

C. Uncertainty Budget for Luminous Intensity Measurements

In Table 3 the uncertainties for luminous intensity measurement of inside-frosted lamps are summarized. The starting point is the uncertainty budget in Table 2; u_c for the illuminance responsivity of a photometer, 0.19%, carries over directly and becomes the dominant uncertainty in this budget. Nevertheless the errors in the calibrations of the eight photometers were reduced by an intercomparison. All photometers were used to measure five lamps. A correction factor was applied to each calibration to maximize the self-consistency among the 40 measurements, with a constraint that the product of the factors was 1. The average change was 0.13%, and the residual scatter was 0.02%, which is the measurement noise of a single photometer measuring a single lamp. While this indicates an additional random error in the individual calibrations of unknown origin, after eight calibrations were averaged the remaining uncertainty resulting from random effects is less than that predicted in Table 2.

The photometers are operated through three cycles of exposure and darkness. Each period of exposure or darkness lasts ~3 s, including settling time and an integration time of 1.67 s for the output voltage measurement. This provides sufficient noise reduction yet is sufficiently quick to obviate worry about heating the filter because of optical absorption, a mechanism that would not be detected by the temperature probe, is quickly avoided. While a precise model would depend on detailed knowledge about the construction of the filters, we estimate that the influence of absorption on one measurement is $< 0.002\%$. While any short-term drift of the photometer cannot be attributed to absorption by the filter at these power levels, errors might arise at higher irradiances or with longer integration times.

The uncertainty of the photometer to lamp distance, r in Eq. (8), is discussed in detail in Subsection 2.B. The various geometrical uncertainties make negligible contributions to the overall uncertainty. A transverse misalignment of the photometer by ± 2 mm would affect the measurement by parts in 10^7. A nonorthogonality to the longitudinal axis of 5 mrad would affect the measurement by $< 0.002\%$. Clearly the geometrical prerequisites of Eq. (8) are met. The angles of incidence on the photometer from the extended source are much less than those encountered during illuminance calibration, and this would tend only to reduce the systematic error in the numerical aperture already accounted for.

NIST originally elected to use inside-frosted lamps as luminous intensity standards because measurement results were less affected by small changes in the orientation of the lamps.[36] Variations of $< 0.2\%$ were reported for misorientations in pitch (about the vertical lamp axis) of less than $\pm 2°$. Similarly the fine-grained frosting aids in generating uniform illu-

Table 3. Uncertainty Budget for Luminous Intensity Measurements

Measurable	Uncertainty Origin	Uncertainty (%) Type A	Uncertainty (%) Type B
Illuminance responsivity			
	Scale uncertainty from Table 2		0.19
	Measurement noise	0.02	
	Filter absorption		0.002
Lamp-to-photometer distance			
	Size and construction of lamp		0.06
	Physical distance measurement	0.01	
Geometrical			
	Photometer transverse placement		[a]
	Photometer orthogonality		0.002
Lamp operation			
	Current regulation		0.03
	Aging (per hour)		0.1
Combined standard uncertainty		0.23	
Expanded uncertainty ($k = 2$)		0.46	

[a]Too small to list.

minance in the far field in the neighborhood of the photometer. We believe that any remaining local variations in illuminance will not contribute to measurement error beyond those already accounted for in connection with the spatial averaging of the responsivity of the photometers. Errors that may arise because of the differences in lamp orientation between NIST and other laboratories are beyond the scope of this paper.

At the operating point, marginal fractional changes in lamp current cause magnified fractional changes in lamp output by factors of 6 (Ref. 37) to 8 (Ref. 14). The standard uncertainty in the budget of 0.03% arises from the 0.15-mA resolution in the control of a 3-A filament current and from the calibration uncertainty of the shunt resistor.

Before luminous intensity measurements were made, the lamp currents were ramped slowly up to the operating point, and the lamps were permitted an equilibration time of at least 10 min. Nevertheless it is important to remember that lamps change with age rather than reach a stable equilibrium. Figure 7(a) shows the behavior of three types of lamp over the course of 2 h of operation. Figure 7(b) demonstrates that the effect spans separate lamp lightings. The gaps in the data correspond to ramping and equilibration periods during which no data were taken. While Fig. 7(a) shows that the lamps changed most rapidly for an additional 20–30 min after the initial warm-up period (as noted above in connection with the r_0 determination), permanent changes in luminous intensity of 0.1%/h contraindicate long equilibration times and are a severe limitation on a calibration service requiring lamps as transfer standards.

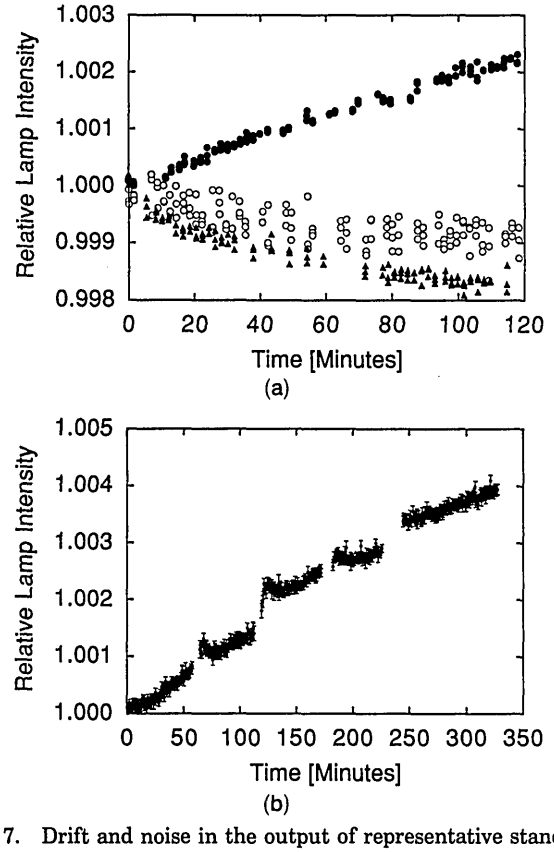

Fig. 7. Drift and noise in the output of representative standard lamps: (a) During one lighting of an Osram Wi 41/G lamp, ●; a FEL, ○; and an inside-frosted T-20 lamp, ▲. (b) During five consecutive lightings of the Osram lamp.

E. Comparison of New and Old Scales

Before this study the last full realization of the old luminous intensity scale occurred in 1985 in connection with the international intercomparison of such scales.[38] At that time the NBS candela was found to be 0.58% smaller than the world mean. (That is, lamps calibrated at NBS were given higher candela values than the average.) Of this, 0.35% was later removed with the adoption of ITS-90,[10] putting the NIST scale 0.23% smaller than the world mean.

Early tests showed that a detector-based candela, when photometers similar to those reported in this study were used, gave results 0.07% above the world mean. This was determined by measuring the primary lamp group with the prototype photometers. In the subsequent two years, two of these prototype photometers were used to measure the same lamps twice again. The original difference of 0.65% narrowed to 0.14%, which indicated that the accuracy of the scale was still within tolerance and that, if drift was due solely to the aging of the lamp group, the scale realization was drifting closer toward the world mean.

A definitive comparison between the old candela scale and the new involves contemporaneous use of the alternative methods. A comparative study of the two scales has begun and will be reported at a later date. Based on the information to date, we believe that the present study does not cause a significant scale shift within the uncertainty of the old scale; it will be perhaps of the order of 0.3%.

5. Conclusion

Two major goals have been reached. A luminous intensity scale has been realized with detectors in a simpler and more direct manner than before. In the process the uncertainty of lamp calibration has been reduced.

This change also puts NIST on good footing for future improvements. The principal uncertainties in the illuminance calibration, the uncertainty of the spectral response scale and the uncertainty in the aperture area, will be reduced significantly by ongoing research and development in our Division. We can expect to reduce the smaller uncertainties as well by improvements in measurement technique. A 0.2% expanded uncertainty in illuminance measurement appears to be achievable.

This study will be of particular benefit for those many applications where illuminance needs to be measured directly, including imaging (such as photography) and ergonomics, where the effects of lighting rather than the light sources themselves matter. Based on our experience with the prototype photome-

ters over the course of three years, we believe that the detector-based scale will prove more durable and stable than the lamp-based scale. This opens the possibility that NIST may offer calibration services based on standard photometers (calibrated for lux) in addition to standard lamps (calibrated for candela).

While traditional photometry has always involved standard light sources, e.g., lamps in recent decades, detector-based standardization permits better accuracies and often simpler procedures. Unlike lamps the photometers require no large power supplies, and they are useful over a wide dynamic range. Photometry benches need not be long to provide for $1/r^2$ attenuations. Well-characterized photometers should prove especially useful for the calibration of modern, nonincandescent light sources, including self-luminous displays. (Care needs to be taken to know the spectrum of the source.) Stable photometers also permit the incidental use of lamps during calibration procedures without regard to their long-term stability. With standard quality lamps becoming more difficult to procure, this alternative technology merits particular attention.

Many people, staff and visitors, contributed much to this project. We thank Ron Wilkinson for many skilled photometric measurements; Joel Fowler and Pat Tobin for much assistance in the design and construction of the new bench; H. Sun for many filter characterizations and extensive study of the temperature dependence of the photometers; John Jackson for measuring the spectral irradiance of lamps at the NIST Facility for Automated Spectroradiometric Calibrations; George Andor, Don McSparron, and Ed Zalewski for the prior work on detector-based photometry; Donna Bell and Jason Hoffman for able assistance in many respects; Bob Saunders for many helpful discussions; and Klaus Mielenz for support and encouragement throughout the project.

Address correspondence to J. Hardis: (301) 975-2373; hardis@vax844.phy.nist.gov.

References and Notes

1. J. W. T. Walsh, *Photometry,* 3rd ed. (Constable, London, 1958), Chap. 1.
2. *Comptes Rendus des Séances de la Neuvième Conférence Générale des Poids et Mesures* (Bureau International des Poids et Mesures, Paris, 1949), session 9, p. 53.
3. W. R. Blevin and B. Steiner, "Redefinition of the candela and the lumen," Metrologia **11,** 97–104 (1975).
4. *Comptes Rendus des Séances de la 16e Conférence Générale des Poids et Mesures* (Bureau International des Poids et Mesures, Sèvres, France, 1979), session 16, p. 100; see also P. Giacomo, "News from BIPM," Metrologia **16,** 55–61 (1980) [corrected English translation **17,** 74 (1981)].
5. R. L. Booker and D. A. McSparron, *Photometric Calibrations,* Natl. Bur. Stand. (U.S.) Spec. Publ. **250-15** (1987).
6. J. H. Walker, R. D. Saunders, and A. T. Hattenburg, "The NBS scale of spectral radiance," Metrologia **24,** 79–88 (1987); *Spectral Radiance Calibrations,* Natl. Bur. Stand. (U.S.) Spec. Publ. **250-1** (1987).
7. J. H. Walker, R. D. Saunders, J. K. Jackson, and D. A. McSparron, *Spectral Irradiance Calibrations,* Natl. Bur. Stand. (U.S.) Spec. Publ. **250-20** (1987).
8. The present study follows, to the extent possible, *Guide to the Expression of Uncertainty in Measurement,* soon to be made final by the International Organization for Standardization, Geneva. NIST has decided to conform to the Guide in all activites by 1994, using an expanded uncertainty coverage factor (as defined in the Guide) of $k = 2$. Earlier studies at NIST were generally reported with 3σ uncertainties. For consistency in this paper, when a standard uncertainty of the present study is compared with an earlier result, the latter is restated to a 1σ basis. Earlier results are restated to a 2σ basis when the context calls for an expanded uncertainty; see also B. N. Taylor and C. E. Kuyatt, *Guidelines for Evaluating and Expressing the Uncertainty of NIST Measurement Results,* Natl. Inst. Stand. Tech. Tech. Note **1297** (1993).
9. H. Preston-Thomas, "The International Temperature Scale of 1990 (ITS-90)," Metrologia **27,** 3–10, 10(E) (1990).
10. K. D. Mielenz, R. D. Saunders, A. C. Parr, and J. J. Hsia, "The 1990 NIST scales of thermal radiometry," J. Res. Natl. Inst. Stand. Technol. **95,** 621–629 (1990).
11. K. D. Mielenz, R. D. Saunders, and J. B. Shumaker, "Spectroradiometric determination of the freezing temperature of gold," J. Res. Natl. Inst. Stand. Technol. **95,** 49–67 (1990).
12. G. Wyszecki, W. R. Blevin, K. G. Kessler, and K. D. Mielenz, *Principles Governing Photometry,* (Bureau International des Poids et Mesures, Sèvres, France, 1983); "Principles governing photometry," Metrologia **19,** 97–101 (1983).
13. *The Basis of Physical Photometry,* Publication 18.2 (Commission Internationale de l'Éclairage, Paris, 1983). (Currently available through the U.S. National Committee of the CIE, c/o T. M. Lemons, TLA-Lighting Consultants, Inc., 72 Loring Ave., Salem, Mass. 01970).
14. T. M. Goodman and P. J. Key, *A Radiometric Realization of the Candela,* NPL Rep. QU 75 (National Physical Laboratory, Teddington, UK, 1986); "The NPL radiometric realization of the candela," Metrologia **25,** 29–40 (1988).
15. L. P. Boivin, A. A. Gaertner, and D. S.Gignac, "Realization of the new candela (1979) at NRC," Metrologia **24,** 139–152 (1987).
16. C. Carreras and A. Corrons, "Absolute spectroradiometric and photometric scales based on an electrically calibrated pyroelectric radiometer," Appl. Opt. **20,** 1174–1177 (1981).
17. Z. Gao, Z. Wang, D. Piao, S. Mao, and C. Yang, "Realization of the candela by electrically calibrated radiometers," Metrologia **19,** 85–92 (1983).
18. J. L. Gardner, "Recent international intercomparison of basic lighting standards," Light. Aust. **7**(4), 21–24 (1987).
19. V. I. Sapritskii, "A new standard for the candela in the USSR," Metrologia **24,** 53–59 (1987); "National primary radiometric standards of the USSR," Metrologia **27,** 53–60 (1990).
20. V. Jediny, J. Krempasky, J. Zatkovic, and P. Nemecek, "Luminous intensity measurement according to the new definition of the candela," Cesk, Cas. Fys. A **38**(6), 601–611 (1988).
21. G. Eppeldauer, "Longterm changes of silicon photodiodes and their use for photometric standardization," Appl. Opt. **29,** 2289–2294 (1990).
22. *Methods of Characterizing the Performance of Radiometers and Photometers,* Publ. 53 (Commission Internationale de l'Éclairage, Paris, 1982) (see Ref. 13 for availability).
23. G. Eppeldauer and J. E. Hardis, "Fourteen-decade photocurrent measurements with large-area silicon photodiodes at room temperature," Appl. Opt. **30,** 3091–3099 (1991).
24. G. Eppeldauer, "Temperature monitored/controlled silicon photodiodes for standardization," in *Surveillance Technologies,* S. Gowrinathan, R. J. Mataloni, and S. J. Schwartz, eds., Proc. Soc. Photo-Opt. Instrum. Eng. **1479,** 71–77 (1991).
25. E. F. Zalewski and C. R. Duda, "Silicon photodiode device with 100% external quantum efficiency," Appl. Opt. **22,** 2867–2873 (1983).

26. The characteristics of the same model of monochromator are described in R. D. Saunders and J. B. Shumaker, "Apparatus function of a prism-grating double monochromator," Appl. Opt. **25,** 3710–3714 (1986).
27. Hamamatsu Corporation, P.O. Box 6910, Bridgewater, N. J. 08807-0910; specific firms and trade names are identified in this paper to specify the experimental procedure adequately. Such identification does not imply recommendation or endorsement by the National Institute of Standards and Technology, nor does it imply that the materials or equipment identified are necessarily the best available for the purpose.
28. The authors extend special thanks to Phil Boivin, National Research Council of Canada, and David Nettleton, National Physical Laboratory of Great Britain, for kindness and generosity in supplying some of the filters used in this project. We also thank G. Czibula, PRC Krochmann (Geneststrasse, 6, D-1000 Berlin 62, Germany), for cooperation and assistance in developing the additional filters.
29. G. Czibula, "Producing a detector with predetermined spectral responsivity," presented at the International Measurement Confederation 10th International Symposium of the Technical Committee on Photo-Detectors, 20–22 September 1982, Berlin.
30. T. M. Goodman, J. E. Martin, B. D. Shipp, and N. P. Turner, "The manufacture and measurement of precision apertures," in *Proceedings of the Second International Conference on New Developments and Applications in Optical Radiometry,* M. P. Fox and D. H. Nettleton, ed., Vol. 92 of Institute of Physics Conference Series (Institute of Physics, Bristol, UK, 1989), pp. 121–128.
31. View Engineering, 1650 N. Voyager Ave., Simi Valley, Calif. 93063.
32. P. Giacomo, "News from the BIPM," Metrologia **17,** 69–74 (1981); see also H. H. Ku, *Uncertainty and Accuracy in Physical Measurements,* Natl. Inst. Stand. Tech. Spec. Publ. **805** (1990).
33. C. L. Cromer, "A new spectral response calibration method using a silicon photodiode trap detector," presented at the 1991 Measurement Science Conference.
34. K. L. Eckerle, J. J. Hsia, K. D. Mielenz, and V. R. Weidner, *Regular Spectral Transmittance,* Natl. Bur. Stand. (U.S.) Spec. Publ. 250-6 (1987).
35. Leeds & Northrup, North Wales, Pa. 19454.
36. E. F. Zalewski, A. R. Schaefer, K. Mohan, and D. A. McSparron, *Optical Radiation Measurements: Photometric Instrumentation and Research (1970 to 1971),* Natl. Bur. Stand. (U.S.) Tech. Note 594-2, 22–33 (1972).
37. *Incandescent Lamps,* Publication TP-110 (General Electric Company, Nela Park, Cleveland, Ohio, 1964).
38. J. Bonhoure, Metrologia **24,** 157–162 (1987); *Rapport de la 11e Session, Comité Consultatif de Photométrie et Radiométrie* (Bureau International des Poids et Mesures, Sèvres, France, 1986).
39. Andor and Zakewski, (personal communication).